

# Integrating Global Gene Expression and Radiation Survival Parameters across the 60 Cell Lines of the National Cancer Institute Anticancer Drug Screen

Sally A. Amundson,<sup>1,2</sup> Khanh T. Do,<sup>2</sup> Lisa C. Vinikoor,<sup>2</sup> R. Anthony Lee,<sup>2</sup> Christine A. Koch-Paiz,<sup>2</sup> Jaeyong Ahn,<sup>1</sup> Mark Reimers,<sup>3,5</sup> Yidong Chen,<sup>4</sup> Dominic A. Scudiero,<sup>6</sup> John N. Weinstein,<sup>3</sup> Jeffrey M. Trent,<sup>7</sup> Michael L. Bittner,<sup>7</sup> Paul S. Meltzer,<sup>4</sup> and Albert J. Fornace, Jr.<sup>1,8</sup>

<sup>1</sup>Center for Radiological Research, Columbia University Medical Center, New York, New York; <sup>2</sup>Gene Response Section, <sup>3</sup>Genomics and Bioinformatics Group, Laboratory of Molecular Pharmacology, and <sup>4</sup>Genetics Branch, Center for Cancer Research, National Cancer Institute, NIH, Bethesda, Maryland; <sup>5</sup>Department of Biostatistics, Virginia Commonwealth University, Richmond, Virginia; <sup>6</sup>Science Applications International Corporation, National Cancer Institute, Frederick Cancer Research and Development Center, Frederick, Maryland; <sup>7</sup>Translational Genomics, Phoenix, Arizona; and <sup>8</sup>Department of Biochemistry and Molecular and Cellular Biology, Lombardi Comprehensive Cancer Center, Georgetown University, Washington, District of Columbia

## Abstract

**The 60 cell lines of the National Cancer Institute Anticancer Drug Screen (NCI-60) constitute the most extensively characterized *in vitro* cancer cell model. They have been tested for sensitivity to more than 100,000 potential chemotherapy agents and have been profiled extensively at the DNA, RNA, protein, functional, and pharmacologic levels. We have used the NCI-60 cell lines and three additional lines to develop a database of responses of cancer cells to ionizing radiation. We compared clonogenic survival, apoptosis, and gene expression response by microarray. Although several studies have profiled relative basal gene expression in the NCI-60, this is the first comparison of large-scale gene expression changes in response to genotoxic stress. Twenty-two genes were differentially regulated in cells with low survival after 2-Gy  $\gamma$ -rays; 14 genes identified lines more sensitive to 8 Gy. Unlike reported basal gene expression patterns, changes in expression in response to radiation showed little tissue-of-origin effect, except for differentiating the lymphoblastoid cell lines from other cell types. Basal expression patterns, however, discriminated well between radiosensitive and more resistant lines, possibly being more informative than radiation response signatures. The most striking patterns in the radiation data were a set of genes up-regulated preferentially in the p53 wild-type lines and a set of cell cycle regulatory genes down-regulated across the entire NCI-60 panel. The response of those genes to  $\gamma$ -rays seems to be unaffected by the myriad of genetic differences across this diverse cell set; it represents the most penetrant gene expression response to ionizing radiation yet observed. [Cancer Res 2008;68(2):415–24]**

## Introduction

In the 1980s, the National Cancer Institute (NCI) selected 60 cell lines representing nine tumor types (breast, central nervous system, colon, leukemia, lung, melanoma, ovarian, prostate, and renal) and established the NCI-60 panel of cancer cell lines as a tool

**Note:** Supplementary data for this article are available at Cancer Research Online (<http://cancerres.aacrjournals.org/>).

**Requests for reprints:** Sally A. Amundson, Center for Radiological Research, Columbia University Medical Center, 630 West 168th Street, VC11-215, New York, NY 10032. Phone: 212-305-3911; Fax: 212-605-3229; E-mail: [saa2108@columbia.edu](mailto:saa2108@columbia.edu).

©2008 American Association for Cancer Research.  
doi:10.1158/0008-5472.CAN-07-2120

for *in vitro* drug screening. Data from the NCI-60 screen have led to identification of mechanisms of drug action, approval of new chemotherapy drugs (e.g., bortezomib), and basic advances in the understanding of cancer mechanisms (1–3). Continued screening of potential chemotherapy agents and molecular characterization of the cell lines make this information-rich system a valuable resource (4).

We began early gene expression studies in the NCI-60 with the measurement of  $\gamma$ -ray induction of three genes (5). That study illustrated the potential for mechanistic insight based on hypotheses generated from complex data sets. The study identified a subset of p53 wild-type cell lines with defective *GADD45A* induction by  $\gamma$ -rays. The drug sensitivity database revealed the same cell lines to be significantly resistant to topoisomerase II inhibitors, leading to the ultimate elucidation of a role for Gadd45 in regulating accessibility of damaged chromatin (6). In a subsequent study (7), we analyzed basal expression levels of 10 genes in the NCI-60 cell lines, finding a striking overall correlation between sensitivity to 122 chemotherapy agents and expression levels of *BCL2L1* (*BCL-XL*). The correlation was independent of growth rate and TP53 status.

More recent studies have compared basal gene expression patterns across the NCI-60 panel using real-time PCR (8) and microarrays (9–14). Those studies found that several of the original tissue-of-origin designations seemed to be incorrect. The tissue type designations used in this article have been updated accordingly. MDA-MB-435 and its ERBB2 transfectant, MDA-N, originally in the breast cancer panel, are now classified as melanoma cell lines (9, 10). Spectral karyotyping has identified NCI/ADR, a presumptive breast cancer line, as an ovarian line derived from OVCAR8 (15, 16).

Most studies of gene expression in the NCI-60 have focused on basal expression levels. In contrast, our studies have focused on the gene expression response to stress. We have applied both quantitative single gene approaches (7, 17) and microarray profiling to study ionizing radiation (18–20) and other stresses (21, 22) in human cell lines and primary cells (23, 24). Those studies revealed an extremely heterogeneous response to radiation among different cell lines. We speculated that the response of specific genes to ionizing radiation might correlate with radiation sensitivity across the genetically diverse NCI-60. Identification of such genes could lead to development of useful biomarkers for monitoring the progress of radiation therapy and for predicting therapeutic effectiveness.

Here, we present (a) the first microarray studies of gene expression changes in the NCI-60 (and three additional lymphoblastoid/myeloid cell lines) in response to ionizing radiation and (b) clonogenic survival experiments that establish radiation survival curves for those cell lines. We have identified 22 genes associated with low survival after 2-Gy  $\gamma$ -rays, 14 genes associated with low survival after 8 Gy, and 25 genes with radiation responses dependent on wild-type p53. The only response common to all 63 of the cell lines studied was the coordinate down-regulation of a set of mitosis-associated genes, possibly regulated by E2F4 and RBL2. The strongly conserved regulation of those genes across all mutational backgrounds and tissues of origin suggests a central role in radiation response that should be explored more fully.

## Materials and Methods

**Cell culture and irradiation.** Cell lines from the NCI-60 panel (2, 25) were obtained from the NCI/Frederick Cancer Research Facility and grown in RPMI 1640 supplemented with 10% fetal bovine serum. All cultures were maintained at 37°C in a humidified 5% CO<sub>2</sub> atmosphere and tested periodically to ensure absence of *Mycoplasma*. Suspension lines were maintained between 1 and 12 × 10<sup>5</sup> cells/mL and were irradiated in log phase at 4 × 10<sup>5</sup> to 5 × 10<sup>5</sup> cells/mL. Nonsuspension lines were irradiated at 60% to 70% confluence. All cultures were fed with fresh medium the day before treatment. Cultures were treated with 0 Gy (mock irradiated) or with 1- to 16-Gy  $\gamma$ -radiation delivered at 2.9 Gy/min with a Mark I-68 <sup>137</sup>Cs source (J.L. Shepherd and Associates, Inc.).

**Clonogenic survival.** Cells were plated in duplicate p100 dishes at appropriate dilutions, irradiated, and incubated for colony formation. Colonies were fixed with 70% ethanol and stained with crystal violet, and colonies of >50 cells were counted. Suspension cells were plated in 96-well microtiter plates and clonogenic survival was calculated using Poisson statistics as described (26).

**Caspase activation.** Cells were exposed to 0, 8, or 16 Gy of  $\gamma$ -rays and incubated for 24 h. Aliquots of 10<sup>5</sup> cells were used to measure caspase activity using the CaspSCREEN Flow Cytometric Apoptosis Detection Kit (BioVision) following the manufacturer's recommendations.

**RNA extraction and microarray hybridization.** After irradiation, cultures were incubated for 4 h, and RNA was extracted using a modified guanidine thiocyanate method followed by purification with RNeasy columns (Qiagen). Whole-cell RNA (80–100  $\mu$ g) was labeled and hybridized to 6,727-element microarrays, as previously described (18). In brief, probes were PCR amplified from IMAGE consortium clones and arrayed on poly-L-lysine-coated glass slides. Fluorescence-labeled cDNA was prepared from RNA by a single round of reverse transcription (Superscript II, Invitrogen) in the presence of Cy3-dUTP or Cy5-dUTP (NEN). Probes and targets were hybridized together for 16 to 18 h in 3× SSC at 65°C in the presence of human CoT1 DNA, yeast tRNA, and polydeoxyadenine. Hybridized slides were washed twice in 0.5× SSC, 0.01% SDS for 5 min, and once in 0.06× SSC for 5 min. The fluorescence signals from Cy3 and Cy5 were scanned with a laser confocal scanner (Agilent Technologies) and images were analyzed with the ArraySuite 2.1 extensions in the IPLab program (Scanalytics, Inc.) to calibrate relative ratios and confidence intervals for their significance (27). The ArraySuite analysis incorporates four separate metrics of hybridization quality for each target, taking into account the intensity, background, and other characteristics of each spot for both fluorochromes. An overall quality assessment was generated for each target on the array (28) and used for data filtering. The ratios were normalized to a set of 88 internal controls with low variation in expression across many kinds of samples (29). The variance in this housekeeping set was used to determine the significance of expression changes following irradiation. Up-regulation and down-regulation were called at the level of 99% confidence. The microarray data have been deposited in National Center for Biotechnology Information

Gene Expression Omnibus (accession no. GSE7505),<sup>9</sup> in the NCI Developmental Therapeutics Program database,<sup>10</sup> and in CellMiner,<sup>11</sup> a relational database developed for integrative analysis of the NCI-60 profiles at the DNA, RNA, protein, chromosomal, and pharmacologic levels.

Gene selection and cluster analysis of the log 2-normalized microarray data were done using the National Human Genome Research Institute online microarray analysis tools developed jointly with Center for Information Technology, NIH. Cell lines were ranked by the radiation response parameters (Table 1) and sensitive or resistant lines for each parameter were defined by cutting the groups at discontinuities in the data. The sensitive or resistant groups comprised between 11 and 21 cell lines (mean, 16). For each parameter, weighted gene analysis (30, 31) was used to identify genes with significantly different responses in the two groups, as assessed using four different separation metrics: maximum pairwise *t* statistic, distance-based method, Wilcoxon/Kruskal-Wallis statistic, and class correlation. For each parameter, statistical significance was calculated by permuting the sample class labels 10,000 times. Only genes with discriminative power greater than any occurring in the random permutation test using three of the four metrics were included in the final gene sets (21).

**Single-probe hybridizations.** Serial dilutions of RNA were immobilized on nylon membranes, hybridized with cDNA probes at 52°C in Hybrisol I (Chemicon), and washed under standard conditions. Hybridization was quantitated on a phosphorimager (Molecular Dynamics), and relative signal levels, normalized to the polyadenylate content of each sample, were determined using the RNA-Think program (32). With that approach, the values for relative RNA levels are directly proportional to RNA abundance, and differences  $\geq$ 1.5-fold can be identified reliably.

**Mitotic index by flow cytometry.** TK6 and NH32 cells were irradiated in exponential phase, and colcemid was added 2 h before fixation of the cells for collection of mitoses. Aliquots of 2 × 10<sup>6</sup> cells were fixed at –20°C in 70% ethanol at times between 4 and 24 h after irradiation, permeabilized, and stained with Alexa 647–conjugated histone H3 pS28 antibody (BD PharMingen) following the protocol of the supplier. Cells were resuspended in propidium iodide (5  $\mu$ g/mL) and RNase A (10  $\mu$ g/mL) and run on a FACSCaliber flow cytometer (Becton Dickinson). At least 20,000 cells were collected for each point, and mitotic index was scored as the percentage of cells with G<sub>2</sub> DNA content staining positive for phospho-histone H3.

**Immunofluorescence.** For *in situ* detection of E2F4, cells were grown and irradiated on chamber slides, fixed in 2% paraformaldehyde, and exposed to E2F4 primary antibody (MAB8894, Chemicon) followed by an Alexa 488–conjugated secondary antibody (Invitrogen) using standard protocols. Slides were counterstained with propidium iodide and images were captured with a Nikon D-Eclipse C1 confocal microscope to allow scoring of at least 100 cells per point in each of three independent experiments. For individual cells, average E2F4 fluorescence intensity in the nuclear area (propidium iodide-stained) was quantified with IPLab image analysis software (Scanalytics, Inc.) and normalized to the overall E2F4 fluorescence intensity of the entire cell.

## Results

**Clonogenic survival and apoptosis following exposure to radiation.** Clonogenic survival after exposure to 0, 2, 5, or 8 Gy of  $\gamma$ -rays was measured for the NCI-60 and three additional cell lines. ML-1, TK6, and NH32 were included in this study because we had used them in many of our prior radiation and gene expression studies (17–20, 22) and they therefore provided a link to those studies. In addition, NH32 is an isogenic derivative of TK6 in which the *p53* gene has been deleted by gene targeting (33). For some cell

<sup>9</sup> <http://www.ncbi.nlm.nih.gov/geo/>

<sup>10</sup> <http://www.dtp.nci.nih.gov>

<sup>11</sup> <http://discover.nci.nih.gov>

lines, dose points at 1 and 6 Gy were added to clarify the shape of the survival curve.  $D_0$  and extrapolation number ( $n$ ), two variables commonly used to describe the shape of survival curves (34), were calculated.  $D_0$  is the dose required to reduce survival by 37% (a factor of  $e$ ) in the linear part of the curve. The extrapolation number, a measure of the initial shoulder of the survival curve, is the  $y$ -intercept obtained by extrapolating the linear part of the curve back to the axis. Surviving fractions at 2 Gy (SF2), 5 Gy (SF5), and 8 Gy (SF8), as well as the calculated parameters, are reported in Table 1.

Caspase activity was determined by flow cytometry as a measure of apoptosis induction. As expected, many of the nonmyeloid/lymphoid cell lines showed little or no apoptotic response in the first 24 h. Caspase activity levels at that time after 8- and 16-Gy  $\gamma$ -ray doses relative to untreated controls are reported in Table 1. Changes of  $\geq 1.9$ -fold were considered significant ( $P < 0.001$ ).

**Microarray analysis.** Gene expression responses to 8 Gy of  $\gamma$ -rays were measured by hybridization to 6,728-element cDNA microarrays. The data were filtered using minimum intensity-of-hybridization and quality control requirements as described in Materials and Methods, yielding a set of 5,186 genes. To reduce noise and lighten the computational load during analyses, that set was further filtered by requiring significant up-regulation or down-regulation (ratios outside the 99% confidence interval of the housekeeping genes on the array) in at least 10% of the cell lines to eliminate the most nonresponsive genes from analysis. That sequence of steps yielded a set of 990 potentially radiation-responsive genes (Supplementary Table S1) that was used in subsequent analyses.

**Gene expression responses by tissue of origin.** Basal gene expression levels in the NCI-60 cell lines were previously found to be strongly correlated with the tissue of origin (9, 14). Although the use of untreated controls for each cell line to obtain response ratios should have removed the basal tissue-of-origin effect, the response to radiation could still have differed between cell lines originating from different tissues. We therefore examined the radiation response data for such a tissue-dependence. In contrast to basal gene expression, the changes in expression in response to radiation did not differ coherently as a function of tissue of origin. The clearest tissue-specific signature was for cells of lymphoid/myeloid origin. Weighted gene analysis (30, 31) was used to identify a set of 21 radiation-responsive genes [false discovery rate (FDR), 4.3%] that discriminated between those cell lines and all others (Table 2). That gene set included only genes with significantly different radiation response ratios (empirical  $P < 0.005$ ) in the two groups as determined by at least three of the four test methods (maximum pairwise  $t$  statistic, distance-based method, Wilcoxon/Kruskal-Wallis statistic, and class correlation).

**Gene responses and p53 status.** Because p53 status is known to be a major determinant of gene expression responses to ionizing radiation, we next looked for genes that responded differently in the p53 mutant and wild-type lines. We identified 25 radiation-responsive genes that were dependent on p53 status across the 63 lines studied (FDR, 1.6%; Fig. 1A). Multidimensional scaling (MDS) based on that set of genes produced a clear grouping of the p53 wild-type lines (Fig. 1B). A literature search revealed that 15 of the 25 genes identified have previously been reported to respond to ionizing radiation in a p53-dependent manner. We then used the p53 wild-type cell line TK6 and its p53-null derivative, NH32, to confirm both the radiation induction and dependence on p53 status of *PHLDA3* and *PLK3* (Fig. 1C), two of the radiation-responsive genes from the p53-discriminating signature.

We also looked for effects of p53 status on radiation sensitivity by comparing the SF2 and SF8 in the p53 wild-type and mutant cell lines (Fig. 1D). Survival did not differ significantly with p53 status at either 2 Gy (Welch's  $t$  test,  $P = 0.23$ ) or 8 Gy (Welch's  $t$  test,  $P = 0.56$ ).

**Radiation sensitivity and gene expression.** We next looked for gene expression signatures related to measurements of radiation sensitivity, identifying 22 genes (FDR, 4.2%) that distinguished the cell lines with low survival following exposure to 2-Gy  $\gamma$ -rays (SF2 < 0.2). Fourteen genes (FDR, 10%) predicted low survival following 8 Gy (SF8 < 0.001), five of those also being in the SF2 gene set. For  $D_0$ , we found only seven genes (FDR 13.3%) that predicted radiation sensitivity ( $D_0 < 90$  cGy). Five of those genes were also in the SF2 set. The findings are summarized in Table 2, where overlap with genes in the lymphoid cell line response signature is also indicated.

In contrast to sensitivity, the only parameter for which genes were found to predict the more resistant cell lines was the extrapolation number ( $n$ ). As a measure of the shoulder on the survival curve, a large  $n$  is generally held to represent higher levels of DNA repair. We found 18 genes (Supplementary Table S2; FDR, 10.6%) for which increased expression after irradiation distinguished the cell lines with large shoulders ( $n > 10$ ). Although those genes were not significantly enriched with DNA repair genes, it was notable that the known X-ray damage repair gene *XRCC1* was selected at the highest level of significance by all methods used.

Other radiation response parameters from Table 1 [caspase activation, doubling time, and  $G_2$  checkpoint deficit from O'Connor et al. (35)] were tested for predictive genes. No genes were identified by more than two statistical methods as significantly distinguishing cell lines with high or low measurements for any of those parameters.

**Coordinate decreased expression of mitosis-associated genes.** Although no genes were up-regulated by ionizing radiation across all of the diverse cell lines in this study, a cluster of genes was broadly down-regulated across essentially the entire panel (Fig. 2A; Supplementary Table S3; Supplementary Fig. S1). Gene Ontology analysis of the genes in that cluster using the EASE algorithm (36) revealed a highly significant overrepresentation of genes involved in mitosis (Bonferroni-corrected EASE score,  $1.8 \times 10^{-22}$ ), cytokinesis ( $2.9 \times 10^{-12}$ ), mitotic spindle components ( $8.2 \times 10^{-6}$ ), and protein serine/threonine kinases ( $3.2 \times 10^{-4}$ ).

We compared the effects of 8 Gy of  $\gamma$ -rays on mitotic index and expression of several of the genes from the down-regulated cluster (*PLK1*, *AURKA*, *CENPA*, and *PPP2R5A*). Within 4 h of radiation exposure, there was a rapid reduction in mitotic index and in expression of all four genes. Gene expression then recovered rapidly, and by 24 h after exposure, all four genes were expressed at or near pre-exposure levels. In contrast, the mitotic index of the cells remained strongly suppressed (Fig. 2B).

We next searched the BIND protein interaction database to retrieve all reported interactions involving the products of the genes in the down-regulated cluster and constructed a Cytoscape interaction map (ref. 37; Fig. 2C). The map revealed a large potential regulatory node containing many of the most strongly and consistently suppressed genes (marked region in Fig. 2A). A majority of those genes have reported interactions with the E2F4 and RBL2 transcription factors, and many also with E2F1 and TAF1. TAF1 was up-regulated at the mRNA level by microarray in about a quarter of the cell lines.

Western blots showed slight up-regulation of E2F4 protein by ionizing radiation, but the effect was not consistently

**Table 1.** Characteristics and radiation survival of cell lines used in this study

Cell line	Type	p53*	T2*	SF2	SF5	SF8	$D_0$	$n$	Casp 8	Casp 16
BT549	Breast	Mut.	58	0.4	0.05	0.015	1.79	1.03	1.45	1.59
HS578T	Breast	Mut.	57	0.48	0.15	0.035	2.04	1.21	1.8	1.61
MCF7	Breast	W.t.	26	0.77	0.32	0.11	2.75	1.52	3.49	7.17
MDA-MB231	Breast	Mut.	39	0.459	0.094	0.008	1.50	205	1.47	1.42
T47D	Breast	Mut.	53	0.26	0.039	0.0047	1.50	1.03	1.1	1.05
SF-268	CNS	Mut.	34	0.5	0.186	0.0227	0.80	90	1.02	1.08
SF-295	CNS	Mut.	30	0.73	0.214	0.0526	1.44	2.37	2.04	0.47
SF-539	CNS	W.t.	34	0.55	0.215	0.159	3.20	1.01	1.89	1.34
SNB19	CNS	Mut.	35	0.38	0.053	0.002	0.90	12.5	1.75	1.89
SNB75	CNS	Mut.	40	0.71	0.248	0.046	1.75	3.92	1.18	1.13
U251	CNS	Mut.	25	0.467	0.061	0.0072	1.50	1.27	1.17	0.96
COLO205	Colon	Mut.	23	0.048	0.0011	0.0003	0.95	0.52	1.15	4.49
HCC-2998	Colon	Mut.	33	0.67	0.051	0.00045	0.61	241	1.75	1.63
HCT116	Colon	W.t.	18	0.465	0.028	0.0019	1.08	2.85	2.59	3.04
HCT15	Colon	Mut.	21	0.659	0.338	0.2006	4.80	0.98	0.46	1.42
HT29	Colon	Mut.	20	0.74	0.5	0.332	7.25	0.99	1.93	2.17
KM12	Colon	Mut.	23	0.505	0.093	0.0038	0.90	24	1.57	0.73
SW620	Colon	Mut.	21	0.58	0.0758	0.000251	0.52	1030	1.04	1.25
A549	Lung	W.t.	24	0.68	0.25	0.05	1.79	4.3	1.26	1.42
EKVX	Lung	Mut.	37	0.94	0.183	0.046	2.00	2.48	2.03	1.33
HOP62	Lung	Mut.	46	0.288	0.091	0.046	2.38	0.49	1.02	1.36
HOP92	Lung	Mut.	88	0.29	0.033	0.00093	0.85	11.6	0.93	1.06
NCI-H226	Lung	Mut.	64	0.631	0.225	0.122	3.70	1.01	1.38	1.42
NCI-H23	Lung	Mut.	37	0.218	0.032	0.0034	1.35	0.97	1.53	1.21
NCI-H322M	Lung	Mut.	37	0.65	0.17	0.008	0.90	27.7	1.68	1.67
NCI-H460	Lung	W.t.	18	0.749	0.601	0.247	6.30	1.07	1.24	0.87
NCI-H522	Lung	Mut.	50	0.43	0.05	0.0026	2.31	2.7	1.26	1.04
CCRF-CEM	Lymphoid	Mut.	27	0.15	0.005	5.96E-05	0.77	2.4	1.42	1.18
HL60	Lymphoid	Mut.	27	0.085	0.0012	0.0000035	0.60	3	1.93	1.24
K562	Lymphoid	Mut.	19	0.0505	0.003	0.00085	1.06	0.33	1.78	2.52
ML-1	Lymphoid	W.t.	24	0.038	0.0011	2.08E-05	0.69	0.5	2.74	1.57
MOLT4	Lymphoid	W.t.	27	0.038	0.0011	0.000021	0.69	0.5	1.47	1.2
NH32	Lymphoid	Mut.	18	0.048	0.0011	0.00011	0.65	0.89	5	3.25
RPMI 8226	Lymphoid	Mut.	31	0.099	0.00188	4.55E-05	0.85	1.08	1.95	1.78
SR	Lymphoid	W.t.	27	0.068	0.00067	7.44E-06	0.75	1.13	1.22	1.91
TK6	Lymphoid	W.t.	15	0.062	0.00086	8.29E-06	0.69	1.1	2.92	3.26
MDA-MB435	Melanoma	Mut.	28	0.57	0.176	0.0083	1.40	3.19	2.92	1.7
MDA-N	Melanoma	Mut.	23	0.7	0.18	0.031	1.71	3.38	1.43	1.88
LOX-IVMI	Melanoma	W.t.	21	0.184	0.031	0.002	1.30	0.99	1.64	1.88
M14	Melanoma	Mut.	27	0.621	0.147	0.018	1.45	4.92	1.32	1.42
MALME-3M	Melanoma	W.t.	35	0.567	0.077	0.002	0.80	34	1.42	1.07
SK-MEL2	Melanoma	Mut.	50	0.48	0.081	0.0065	1.20	2.28	1.02	1.1
SK-MEL28	Melanoma	Mut.	36	0.95	0.31	0.115	2.80	1.88	1.24	1.42
SK-MEL5	Melanoma	W.t.	26	0.852	0.24	0.0995	2.75	1.76	1.97	1.56
UACC-257	Melanoma	W.t.	50	0.51	0.17	0.033	4.75	1.39	3.04	2.22
UACC-62	Melanoma	W.t.	31	0.387	0.035	0.0019	1.00	5.47	1.41	1.81
NCI-ADR	Ovary	Mut.	34	0.561	0.041	0.0071	1.40	2.09	1.1	1.37
IGROV-1	Ovary	W.t.	35	0.389	0.14	0.0603	2.85	0.88	1.7	1.32
OVCAR3	Ovary	Mut.	37	0.577	0.109	0.0145	1.50	2.9	1.56	0.8
OVCAR4	Ovary	W.t.	40	0.241	0.0133	0.00092	1.10	1.15	1.1	2.11
OVCAR5	Ovary	Mut.	55	0.66	0.201	0.0402	1.80	2.94	1.5	1.12
OVCAR8	Ovary	Mut.	25	0.561	0.132	0.0074	1.00	16.1	1.98	1.84
SKOV-3	Ovary	Mut.	57	0.66	0.11	0.021	1.74	2.04	1.34	1.53
DU-145	Prostate	Mut.	37	0.646	0.205	0.0234	1.40	7.6	1.37	1.39
PC3	Prostate	Mut.	39	0.69	0.218	0.0162	1.10	20	1.36	1.26
786-O	Renal	Mut.	23	0.457	0.1027	0.0059	1.00	12	3.22	2.97
A498	Renal	W.t.	65	0.5	0.08	0.0088	1.39	3.17	1.07	1.58

(Continued on the following page)

**Table 1.** Characteristics and radiation survival of cell lines used in this study (Cont'd)

Cell line	Type	p53*	T2*	SF2	SF5	SF8	$D_0$	$n$	Casp 8	Casp 16
ACHN	Renal	W.t.	31	0.648	0.475	0.278	6.20	0.96	2.31	2.31
CAKI-1	Renal	W.t.	38	0.364	0.02	0.0049	1.08	2.28	1.18	1.21
RXF-393	Renal	Mut.	40	0.67	0.315	0.08	2.25	2.63	1.33	1.29
SN12C	Renal	Mut.	30	0.887	0.1903	0.0292	1.65	2.93	1.49	1.52
TK10	Renal	Mut.	34	0.518	0.08	0.0147	1.70	1.66	2.29	1.91
UO31	Renal	W.t.	37	0.477	0.063	0.009	1.50	1.76	1.02	1.22

Abbreviations: CNS, central nervous system; W.t., wild-type TP53 status by sequence; Mut., mutant TP53; T2, doubling time; Casp8 and Casp16, relative caspase activation 24 h after 8 or 16 Gy.

\*Data from ref. 35 except as noted in the text.

reproducible. No changes in protein expression were detected for the other three transcription factors (data not shown). Immunofluorescent staining of E2F4 also showed some increase in expression and a change in intracellular location after irradiation. E2F4 seemed to be predominantly excluded from the

nucleus in unirradiated cells, whereas nuclear staining had markedly increased by 4 h after exposure to 8 Gy (Fig. 2D). The increase in nuclear staining, quantified using IPLab, was significant ( $P < 0.0001$ ) in all cell lines tested (ACHN, HCT116, MCF7, and PC3).

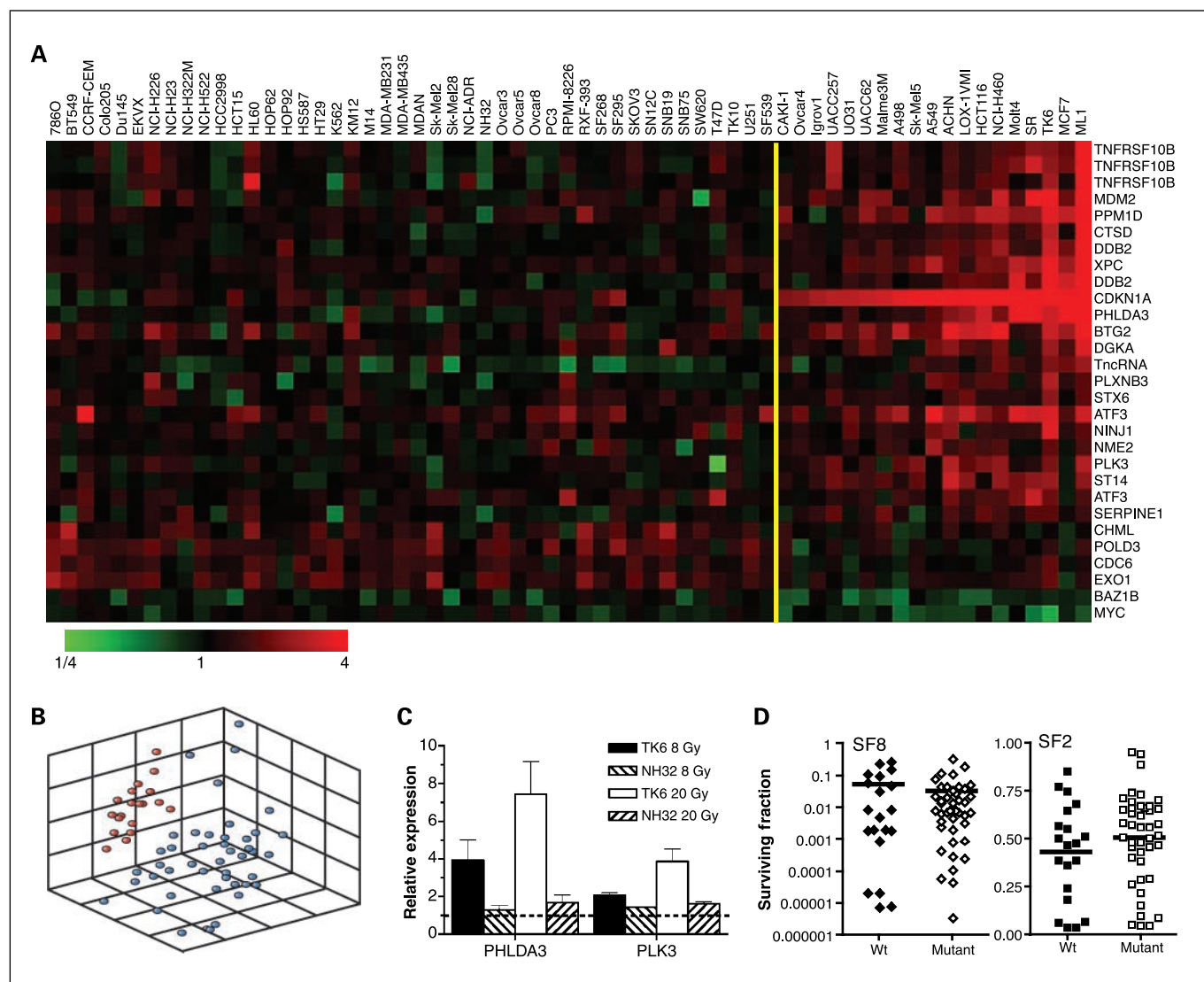
**Table 2.** Summary of radiation-responsive genes in survival (SF2, SF8, and  $D_0$ ) or lymphoblast (Ly) signatures

Image ID	Unigene	Gene	Title	SF2	SF8	$D_0$	Ly
36374	Hs.23960	<i>CCNB1</i>	Cyclin B1	D	D		D
856289	Hs.194698	<i>CCNB2</i>	Cyclin B2	D	D		D
781047	Hs.469649	<i>BUB1</i>	BUB1 budding uninhibited by benzimidazoles 1 homologue (yeast)	D	D	D	D
51448	Hs.460	<i>ATF3</i>	Activating transcription factor 3	Up	Up	Up	Up
744047	Hs.329989	<i>PLK1</i>	Polo-like kinase 1 ( <i>Drosophila</i> )	D	D	D	D
244355	Hs.84	<i>IL2RG</i>	Interleukin 2 receptor, $\gamma$ (severe combined immunodeficiency)	Up	Up		Up
898062	Hs.494347	<i>N/A</i>	Full-length cDNA clone CSODD006YE20 of neuroblastoma	D			D
795877	Hs.398157	<i>PLK2</i>	Polo-like kinase 2 ( <i>Drosophila</i> )	Up			Up
229365	Hs.192039	<i>PTPRC</i>	Protein tyrosine phosphatase, receptor type, C	Up			Up
125134	Hs.243564	<i>CD48</i>	CD48 antigen (B-cell membrane protein)	Up			Up
258120	Hs.522699	<i>COX7B</i>	Cytochrome <i>c</i> oxidase subunit VIIb	Up			Up
788285	Hs.183713	<i>EDNRA</i>	Endothelin receptor type A	Up			Up
264117	Hs.121575	<i>CTSD</i>	Cathepsin D	Up			Up
147075	Hs.567303	<i>MDM2</i>	Mdm2, transformed 3T3 cell double minute 2, p53 binding protein (mouse)	Up			Up
753447	Hs.651197	<i>DDB2</i>	Damage-specific DNA binding protein 2	Up		Up	Up
815774	Hs.75367	<i>SLA</i>	Src-like adaptor	Up			Up
788185	Hs.521456	<i>TNFRSF10B</i>	Tumor necrosis factor receptor superfamily, member 10b	Up		Up	Up
898286	Hs.334562	<i>CDC2</i>	Cell division cycle 2, G <sub>1</sub> to S and G <sub>2</sub> to M		D	D	D
137638	Hs.462693	<i>ZNF22</i>	Zinc finger protein 22 (KOX 15)	Up	Up		
1588935	Hs.268557	<i>PHLDA3</i>	Pleckstrin homology-like domain, family A, member 3	Up	Up		
897690	Hs.192374	<i>HSP90 B1</i>	Heat shock protein 90 kDa $\beta$ (Grp94), member 1	Up	Up		
283715	Hs.304475	<i>LCP2</i>	Lymphocyte cytosolic protein 2		Up		
431655	Hs.166556	<i>CD37</i>	CD37 antigen		Up		
488873	Hs.1501	<i>SDC2</i>	Syndecan 2		Up		
50843	Hs.8086	<i>RNMT</i>	RNA (guanine-7-) methyltransferase		Up		
588453	Hs.153504	<i>TOML1</i>	Target of myb1-like 1 (chicken)	Up			
788256	Hs.270845	<i>KIF23</i>	Kinesin family member 23	D		D	
686081	Hs.402773	<i>PTPN7</i>	Protein tyrosine phosphatase, nonreceptor type 7				Up
701112	Hs.475538	<i>XPC</i>	Xeroderma pigmentosum, complementation group C				Up
549146	Hs.501778	<i>TRIM22</i>	Tripartite motif-containing 22				Up

NOTE: Up or D indicates presence of a gene in the signature, and the direction of change seen in response to radiation.

Abbreviations: Up, up-regulated; D, down-regulated.





**Figure 1.** p53 status and radiation-responsive genes. **A**, heatmap showing fold-change ratios (with and without radiation exposure) for the 25 genes identified as distinguishing p53 status. Cell lines with mutant p53 are to the left of the yellow line, and p53 wild-type lines to the right. **B**, MDS plot showing separation of p53 wild-type (red) and p53 mutant (blue) cell lines by expression of the same 25 genes. **C**, relative  $\gamma$ -ray induction of two genes from the p53 cluster in a p53 wild-type line (TK6) and its p53-null derivative (NH32). Columns, mean of three independent experiments; bars, SE. **D**, distribution of surviving fractions at 8 and 2 Gy as a function of p53 status for all 63 cell lines.

## Discussion

The p53 response has been found to play a central role in most studies of radiation-induced gene expression, making it an important parameter to examine here. Consistent with our previous studies of gene expression after ionizing radiation, the most strongly up-regulated genes in the NCI-60 responded preferentially in p53 wild-type cell lines. Our analysis identified 25 such p53-dependent genes. Many more genes have been reported to be p53 regulated, but it is not surprising that we found only a subset of those. Multiple regulatory factors contribute to gene expression and vary among cell lines, decreasing the ability to see p53 dependence with statistical significance. For example, *GADD45A* is known to be induced by radiation in a p53-dependent manner, but this response is deficient in a subset of NCI-60 lines (5). That heterogeneity of response means that *GADD45A* did not meet the significance requirements for p53-dependent response across the entire cell panel.

One of the most consistently induced genes among the p53 wild-type lines was *PHLDA3*. We have previously observed large inductions of *PHLDA3* in p53 wild-type cells treated with UV radiation (21) and a number of other DNA-damaging agents including ionizing radiation (22). Despite its robust induction in many cell lines, *PHLDA3* has not been previously described as a radiation response gene. We have now confirmed its p53-dependent induction by ionizing radiation. *PHLDA3* has been implicated in apoptosis (38), but its role in radiation response remains uncharacterized.

In different model systems, wild-type p53 has been reported to both increase and decrease radiation sensitivity and clinical response (reviewed in ref. 39). In the sulforhodamine B assay of the NCI-60 screen, wild-type p53 status has also been associated with drug sensitivity for many mechanisms of action but not for antimetotics (4, 35). In the present study, p53 status did not seem to

be a significant determinant of radiation sensitivity in the NCI-60, suggesting that, although manipulations of p53 may alter radiosensitivity in specific model systems, the general loss of p53 in human cancer cells does not contribute consistently to radio-resistance. Tumor cells have evolved diverse survival mechanisms, and many genotypic or phenotypic factors other than p53 likely combine to determine radiosensitivity.

The coordinate down-regulation across the entire NCI-60 panel of genes associated with mitosis was the most striking pattern of gene expression response to ionizing radiation. Because radiation

triggers cell cycle checkpoints to block cells from entering mitosis, the apparent suppression of those genes could simply reflect changes in cell cycle distribution. If such were the case, suppression of mitosis-associated genes might be expected to correlate with growth rate because a greater relative effect should be seen in cell lines normally having a greater proportion of cells in M phase. However, only two of the down-regulated genes, *CCNB1* and *CENPF*, showed significant correlation with doubling time ( $P < 0.01$ ). For all of the other genes in the mitosis cluster, down-regulation by ionizing radiation was independent of doubling time

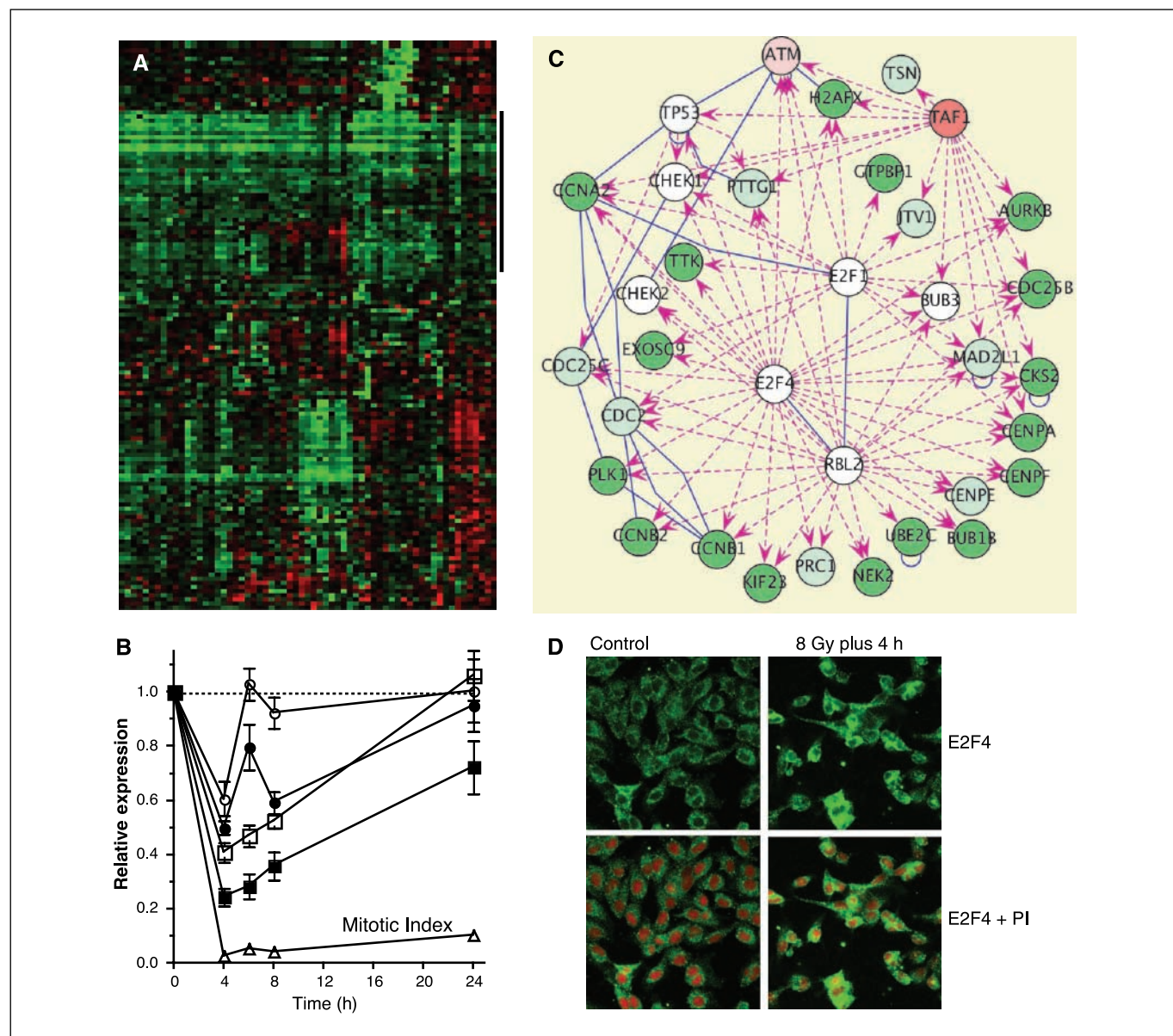


**Figure 2.** Down-regulation of gene expression by ionizing radiation. *A*, heatmap of fold-change ratios for genes significantly down-regulated in >10% of the cell lines. Black bar marks cluster of genes with the most widespread down-regulation. Full annotation is available in Supplementary Fig. S1 and Supplementary Table S3. *B*, relative expression of *PLK1* (■), *AURKA* (□), *CENPA* (●), *PPP2R5A* (○), and mitotic index (△) between 4 and 24 h after exposure to 8-Gy  $\gamma$ -rays. Gene expression was measured by quantitative hybridization; *points*, mean of six independent experiments with TK6 and NH32; *bars*, SE. Data for the two cell lines were combined because there were no apparent differences in response. *Dashed line*, relative levels in untreated controls. *C*, cytoscape interaction map (37) of cluster marked in *A*. *Blue lines*, protein-protein interactions; *arrows*, protein-DNA interactions. *Dark green nodes*, transcripts significantly decreased in at least 25% of the cell lines; *light green nodes*, decrease in >10%; *red nodes*, increased expression in at least 25%; *pink nodes*, increased expression in >10%. *D*, representative staining of E2F4 (green) in ACHN cells 4 h after mock or 8-Gy  $\gamma$ -irradiation. *Bottom*, nuclei counterstained with propidium iodide (red).

(median  $P = 0.33$ ), suggesting that gene regulation, rather than cell cycle redistribution alone, is involved. That suggestion was strengthened by the lack of temporal coupling between changes in mitotic index and expression of genes in the cluster (*PLKL*, *AURKA*, *CENPA*, and *PPP2R5A*). Although gene expression and mitotic index decreased with similar initial kinetics, gene expression levels recovered independently of reentry of cells into M phase. That finding again implies regulation rather than mere loss of cells in mitosis.

Mapping of known DNA interactions with the promoters of the mitosis genes revealed a potential regulatory network centered on the transcription factors E2F4, RBL2, E2F1, and TAF1. TAF1 and E2F1 generally act as activating transcription factors and may participate in normal expression of the mitosis genes in undamaged cycling cells. E2F4 and RBL2 (the p130 retinoblastoma-like protein), however, act together as a repressor complex to prevent gene transcription (40). Hence, they are proteins of particular interest in the context of the down-regulated mitosis gene cluster. The loss or down-regulation of E2F4 also sensitizes cells to killing by chemotherapy agents (41) and radiation (42, 43), further suggesting a role in radiation response.

Induction of E2F4 protein has been reported 8 to 24 h after irradiation of prostate, but not breast cancer, cell lines (42). E2F4 activity can also be regulated by changes in subcellular localization during normal cell cycle progression (44) and in response to ionizing radiation (42, 43). Because gene expression changes in our study were assessed 4 h post-irradiation, we looked for effects on E2F4 at that time. We found significant increases in nuclear E2F4 staining coincident with gene down-regulation in the four cell lines tested. The lack of protein induction in MCF7 cells assayed 24 h after treatment in the prior study contrasts with our finding of nuclear localization and gene down-regulation at 4 h in the same cell line. Protein induction and changes in protein localization do not necessarily represent the same response pathway, however. It seems that nuclear localization and resulting transcriptional suppression represent a conserved early response to radiation damage, whereas changes in protein expression may contribute to later effects and be less tightly conserved among cell lines or tumor types.

Several prior studies have profiled basal gene expression levels in the NCI-60 without genotoxic stress and found correlations with drug sensitivity (10–14) and tissue of origin (9). A recent study of 35 of the NCI-60 lines by Torres-Roca et al. (45) also identified basal gene expression predictors of SF2 values after ionizing radiation. Of the nine genes selected in that study, none were among the 27 radiation response genes that distinguish between sensitive and resistant cell lines across the entire NCI-60 in the present study. This implies that genes with basal expression levels that correlate with radiosensitivity do not necessarily respond to radiation with additional changes in expression levels.

To see how application of our methods to the measured survival and basal data for the whole NCI-60 panel would compare with the previous classifier results (45), Affymetrix U133 measurements of basal expression levels (processed by Robust Multichip Analysis; ref. 14) were subjected to the same analysis as our radiation response data. The same criteria as applied to our radiation data yielded 175 genes that identified cell lines with low SF2 (FDR, 1.8%), 98 for lines with low SF8 (FDR, 1.7%), and 19 for lines with low  $D_0$  (FDR, 2.8%; Supplementary Table S4). Despite the use of very different methods (binary class comparison rather than continuous classifiers and the entire set of 60 cell lines, rather than 35 lines), we

found that three of the nine SF2 classifier genes from Torres-Roca et al. (45), *RPL1A*, *NASP*, and *SFRS1*, were also identified by our SF2 analysis. In contrast, there was no overlap between that previous SF2 classifier and either our SF8 or  $D_0$  basal prediction set. The large number of genes whose basal expression levels are associated with radiation sensitivity parameters and the relatively clear separation of cell lines visualized by MDS (Fig. 3) suggest that profiles of basal gene expression contain as much or more information about radiation sensitivity as do gene expression responses to radiation. That observation is consistent with the finding that basal gene expression often correlates with chemosensitivity (4, 10–12). The two types of measurement are complementary. Basal expression addresses most directly the question of sensitivity and resistance; expression changes in response to a perturbation address most directly the question of downstream consequences.

Because p53 status yielded some of the clearest results with the radiation-response ratio data, we also looked in the U133 data set for genes with basal expression levels that differed as a function of p53 status. In contrast with the radiation survival parameters, for which more genes were identified in the basal expression data set, we identified only two genes (FDR 4.6%), *CDKN1A* and *BAX*, with basal expression that differed as a function of p53. Because not all

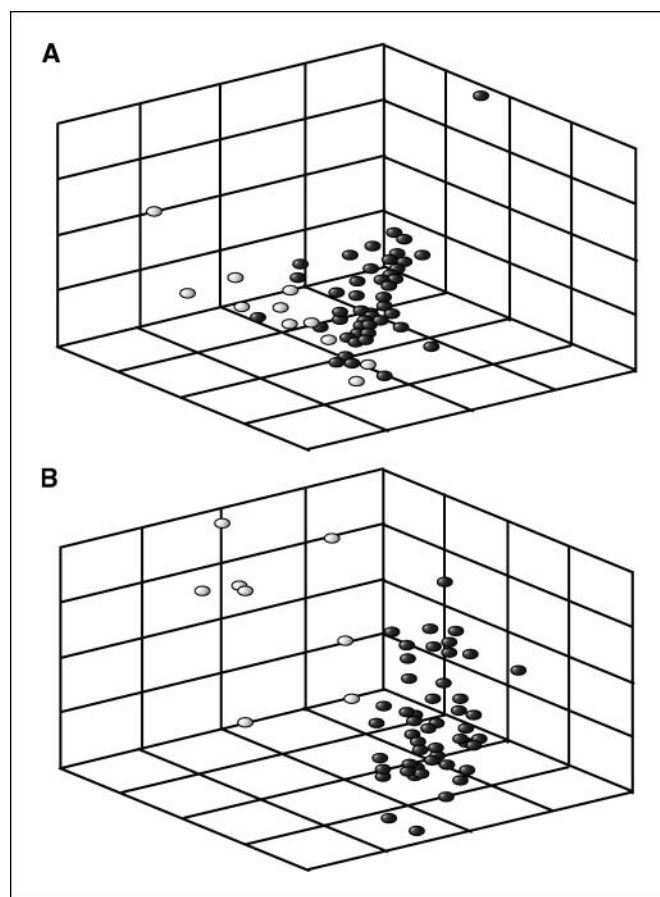


**Figure 3.** A, MDS plot illustrating separation of radiation-sensitive (SF2 <0.2 Gy; red) cell lines from those with SF2 >0.2 Gy (blue) using the 22-gene radiation-response signature. B, MDS plot illustrating separation of radiation-sensitive (SF2 <0.2 Gy; red) cell lines from those with SF2 >0.2 Gy (blue) using the 175-gene basal expression signature.



genes that are radiation inducible by p53 are regulated by p53 in the absence of stress, such a result is not entirely unreasonable. Interestingly, in our earlier study comparing basal expression of 10 genes in the NCI-60 (eight with known p53-dependent stress regulation), we found that only *CDKN1A* ( $P = 0.002$ ) and *BAX* ( $P = 0.003$ ) had basal expression levels correlating significantly with p53 status (7).

Given the strong contribution of basal gene expression levels to cellular radiation response, we wondered if the absolute expression levels post-irradiation would also be informative. We therefore reconstructed approximate post-irradiation levels for the genes present in both our response ratio data and the Affymetrix basal expression data, yielding a set of 4,617 genes. From that set, we were able to identify 31 genes that identified cell lines with SF8 <0.001, and 29 genes that identified lines with SF2 <0.2. Those gene sets did not improve the separation of the groups by MDS, however, and the basal signatures still seemed the most powerful. There was also little overlap between the gene sets selected from the reconstructed values and the corresponding basal or radiation-response ratio sets. Post-irradiation levels of three genes, *CDKN1A*, *BCL2A1*, and *F3*, correlated with p53 status. No relationships could be found between the reconstructed gene expression levels and any of the other parameters tested. It is possible, however, that the amount of noise introduced by merging the two very different types of microarray measurements overwhelmed most structure within the reconstructed data set. The role of absolute post-irradiation gene expression levels in radiation

response will best be determined by direct measurement of such values.

From the present study, it seems that some radiation-induced changes in gene expression can be associated with measured radiation survival parameters but that the basal gene expression pattern before irradiation may be a better predictor of radiation sensitivity. Up-regulation of the p53 pathway represents the most prominent, coherent induced gene pattern in the NCI-60 panel. In contrast, the joint down-regulation of expression of genes involved in mitosis seems to represent a pathway of radiation response broadly conserved among cancer cell lines. Involvement of the E2F4-RBL2 complex as a down-regulator of that pathway suggests that it is an important component, hitherto largely overlooked, of the response to radiation and that it is a possible attractive drug target for enhancement of radiotherapy.

## Acknowledgments

Received 6/7/2007; revised 10/12/2007; accepted 10/30/2007.

**Grant support:** Office of Science (Biological and Environmental Research), U.S. Department of Energy grants DE-FG02-07ER46336 and DE-AI02-02ER63308, and Intramural Research Program of the NIH, National Cancer Institute, Center for Cancer Research.

The costs of publication of this article were defrayed in part by the payment of page charges. This article must therefore be hereby marked *advertisement* in accordance with 18 U.S.C. Section 1734 solely to indicate this fact.

We thank the Division of Computational Bioscience of the Center for Information Technology and the Cancer Genetics Branch of the National Human Genome Research Institute at the NIH for providing computational resources for this study.

## References

- Boyd MR, Paull KD. Some practical considerations and applications of the National Cancer Institute *in vitro* anticancer drug discovery screen. *Drug Dev Res* 1995;34:91-109.
- Shoemaker RH. The NCI60 human tumour cell line anticancer drug screen. *Nat Rev Cancer* 2006;6:813-23.
- Weinstein JN. Spotlight on molecular profiling: "integrated" analysis of the NCI-60 cancer cell lines. *Mol Cancer Ther* 2006;5:2601-5.
- Weinstein JN, Myers TG, O'Connor PM, et al. An information intensive approach to the molecular pharmacology of cancer. *Science* 1997;275:343-9.
- Bae I, Smith ML, Sheikh MS, et al. An abnormality in the p53 pathway following  $\gamma$ -irradiation in many wild-type p53 human melanoma lines. *Cancer Res* 1996;56:840-7.
- Carrier F, Georgel PT, Pourquier P, et al. Gadd45, a p53-responsive stress protein, modifies DNA accessibility on damaged chromatin. *Mol Cell Biol* 1999;19:1673-85.
- Amundson SA, Myers TG, Scudiero D, Kitada S, Reed JC, Fornace AJ, Jr. An informatics approach identifying markers of chemosensitivity in human cancer cell lines. *Cancer Res* 2000;60:6101-10.
- Szakacs G, Annereau JP, Lababidi S, et al. Predicting drug sensitivity and resistance: profiling ABC transporter genes in cancer cells. *Cancer Cell* 2004;6:129-37.
- Ross DT, Scherf U, Eisen MB, et al. Systematic variation in gene expression patterns in human cancer cell lines. *Nat Genet* 2000;24:227-35.
- Scherf U, Ross DT, Waltham M, et al. A gene expression database for the molecular pharmacology of cancer. *Nat Genet* 2000;24:236-44.
- Staunton JE, Slonim DK, Coller HA, et al. Chemosensitivity prediction by transcriptional profiling. *Proc Natl Acad Sci USA* 2001;98:10787-92.
- Annereau JP, Szakacs G, Tucker CJ, et al. Analysis of ATP-binding cassette transporter expression in drug-selected cell lines by a microarray dedicated to multidrug resistance. *Mol Pharmacol* 2004;66:1397-405.
- Huang Y, Anderle P, Bussey KJ, et al. Membrane transporters and channels: role of the transportome in cancer chemosensitivity and chemoresistance. *Cancer Res* 2004;64:4294-301.
- Shankavaram UT, Reinhold WC, Nishizuka S, et al. Transcript and protein expression profiles of the NCI-60 cancer cell panel: an integrative microarray study. *Mol Cancer Ther* 2007;6:820-32.
- Roschke AV, Toton G, Gehlhaus KS, et al. Karyotypic complexity of the NCI-60 drug-screening panel. *Cancer Res* 2003;63:8634-47.
- Bussey KJ, Chin K, Lababidi S, et al. Integrating data on DNA copy number with gene expression levels and drug sensitivities in the NCI-60 cell line panel. *Mol Cancer Ther* 2006;5:853-67.
- Amundson SA, Do KT, Fornace AJ, Jr. Induction of stress genes by low doses of  $\gamma$  rays. *Radiat Res* 1999;152:225-31.
- Amundson SA, Bittner M, Chen YD, Trent J, Meltzer P, Fornace AJ, Jr. cDNA microarray hybridization reveals complexity and heterogeneity of cellular genotoxic stress responses. *Oncogene* 1999;18:3666-72.
- Amundson SA, Patterson A, Do KT, Fornace AJ. A nucleotide excision repair master-switch: p53 regulated coordinate induction of global genomic repair genes. *Cancer Biol Ther* 2002;1:145-9.
- Amundson SA, Lee RA, Koch-Paiz CA, et al. Differential responses of stress genes to low dose-rate  $\gamma$  irradiation. *Mol Cancer Res* 2003;1:445-52.
- Koch-Paiz CA, Amundson SA, Bittner ML, Meltzer PS, Fornace AJ, Jr. Functional genomics of UV radiation responses in human cells. *Mutat Res* 2004;549:65-78.
- Amundson SA, Do KT, Vinikoor L, et al. Stress-specific signatures: expression profiling of p53 wild-type and -null human cells. *Oncogene* 2005;24:4572-9.
- Amundson SA, Shahab S, Bittner M, Meltzer P, Trent J, Fornace AJ, Jr. Identification of potential mRNA markers in peripheral blood lymphocytes for human exposure to ionizing radiation. *Radiat Res* 2000;154:342-6.
- Amundson SA, Grace MB, McLeland CB, et al. Human *in vivo* radiation-induced biomarkers: gene expression changes in radiotherapy patients. *Cancer Res* 2004;64:6368-71.
- Stinson SF, Alley MC, Kopp WC, et al. Morphological and immunocytochemical characteristics of human tumor cell lines for use in a disease-oriented anticancer drug screen. *Anticancer Res* 1992;12:1035-53.
- Furth EE, Thilly WG, Penman BW, Liber HL, Rand WM. Quantitative assay for mutation in diploid human lymphoblasts using microtiter plates. *Anal Biochem* 1981;110:1-8.
- Chen Y, Dougherty ER, Bittner ML. Ratio-based decisions and the quantitative analysis of cDNA microarray images. *J Biomed Opt* 1997;2:364-74.
- Chen Y, Kamat V, Dougherty ER, Bittner ML, Meltzer PS, Trent JM. Ratio statistics of gene expression levels and applications to microarray data analysis. *Bioinformatics* 2002;18:1207-15.
- DeRisi J, Penland L, Brown PO, et al. Use of a cDNA microarray to analyse gene expression patterns in human cancer. *Nat Genet* 1996;14:457-60.
- Bittner M, Meltzer P, Chen Y, et al. Molecular classification of cutaneous malignant melanoma by gene expression profiling. *Nature* 2000;406:536-40.
- Hedenfalk I, Duggan D, Chen Y, et al. Gene-expression profiles in hereditary breast cancer. *N Engl J Med* 2001;344:539-48.
- Koch-Paiz CA, Momenan R, Amundson SA, Lamoreaux E, Fornace AJ, Jr. Estimation of relative mRNA content by filter hybridization to a polyuridylic probe. *Biotechniques* 2000;29:708-14.
- Chuang YY, Chen Q, Brown JP, Sedivy JM, Liber HL. Radiation-induced mutations at the autosomal thymidine kinase locus are not elevated in p53-null cells. *Cancer Res* 1999;59:3073-6.
- Hall EJ. *Radiobiology for the radiologist*. 5th edition. Philadelphia: Lippincott Williams and Wilkins; 2000.

35. O'Connor PM, Jackman J, Bae I, et al. Characterization of the p53 tumor suppressor pathway in cell lines of the National Cancer Institute anticancer drug screen and correlations with the growth-inhibitory potency of 123 anticancer agents. *Cancer Res* 1997;57:4285-300.
36. Hosack DA, Dennis GJ, Sherman BT, Lane HC, Lempicki RA. Identifying biological themes within lists of genes with EASE. *Genome Biol* 2003;4:R70.
37. Shannon P, Markiel A, Ozier O, et al. Cytoscape: a software environment for integrated models of biomolecular interaction networks. *Genome Res* 2003;13:2498-504.
38. Kerley-Hamilton JS, Pike AM, Li N, DiRenzo J, Spinella MJ. A p53-dominant transcriptional response to cisplatin in testicular germ cell tumor-derived human embryonal carcinoma. *Oncogene* 2005;24:6090-100.
39. Cuddihy AR, Bristow RG. The p53 protein family and radiation sensitivity: yes or no? *Cancer Metastasis Rev* 2004;23:237-57.
40. Takahashi Y, Rayman JB, Dynlacht BD. Analysis of promoter binding by the E2F and pRB families *in vivo*: distinct E2F proteins mediate activation and repression. *Genes Dev* 2000;14:804-16.
41. Ma Y, Freeman SN, Cress WD. E2F4 deficiency promotes drug-induced apoptosis. *Cancer Biol Ther* 2004;3:1262-9.
42. DuPree EL, Mazumder S, Almasan A. Genotoxic stress induces expression of E2F4, leading to its association with p130 in prostate carcinoma cells. *Cancer Res* 2004;64:4390-3.
43. Crosby ME, Jacobberger J, Gupta D, Macklis RM, Almasan A. E2F4 regulates a stable G<sub>2</sub> arrest response to genotoxic stress in prostate carcinoma. *Oncogene* 2007;26:1897-909.
44. Verona R, Moberg K, Estes S, Starz M, Vernon JP, Lees JA. E2F activity is regulated by cell cycle-dependent changes in subcellular localization. *Mol Cell Biol* 1997;17:7268-82.
45. Torres-Roca JF, Eschrich S, Zhao H, et al. Prediction of radiation sensitivity using a gene expression classifier. *Cancer Res* 2005;65:7169-76.